International Journal of Thermal Sciences 122 (2017) 248–256

Contents lists available at ScienceDirect

International Journal of Thermal Sciences

journal homepage: www.elsevier.com/locate/ijts

A reactive hydromagnetic heat generating fluid flow with thermal radiation within porous channel with symmetrical convective cooling

A.R. Hassan [a, b, *], R. Maritz [a], J.A. Gbadeyan [c]

[a] Department of Mathematical Sciences, University of South Africa, South Africa
[b] Department of Mathematics, Tai Solarin University of Education, Ijagun, Nigeria
[c] Department of Mathematics, University of Ilorin, Ilorin, Nigeria

ARTICLE INFO

Article history:
Received 3 April 2017
Received in revised form
19 June 2017
Accepted 28 August 2017

Keywords:
Thermal radiation
Convective cooling
Reactive fluid
Hydromagnetic
Padé approximation technique
Heat generation
Porous medium

ABSTRACT

The thermodynamics analysis of a reactive hydromagnetic radiative heat transfer flow within a channel filled with saturated non−Darcy porous medium with convective cooling of the walls is investigated for Arrhenius kinetics. The momentum and energy equations governing the fluid flow are modeled, non-dimensionalised and solved analytically by making use of modified Adomian decomposition Method (MADM). The expressions of momentum and energy profiles are used to analysed the entropy generation rate and the impacts of other flow thermophysical parameters especially the radiative flux on the fluid flow including the thermal stability analysis obtained using Padé approximation technique are presented and discussed.

1. Introduction

Due to the diversity of fluid in nature, studies through investigation explained that lots of models have been proposed to describe fluid behaviour in different circumstances as in Ref. [1]. Studies involving flow of reactive hydromagnetic fluid have been investigated in Refs. [2–8] because of its extensive scope in engineering and industrial applications such as electronic cooling, thermal insulation, crude oil extraction and nuclear reactor. Also, studies involving reacting materials undergoing exothermic reaction and Newtonian cooling where convection forms an integral part of heat transfer due to differences in ambient temperatures as described in Refs. [2–4,9–11]. Meanwhile, the process of convective heat transfer has been examined in several studies mentioned in Refs. [10–16] which involve various flow of fluid between walls with convective cooling effects have been investigated because of its importance in new technological applications, for instance, the cooling processes of nuclear reactor and refrigerators.

Additionally, recent discoveries of magnetic impact on fluid flow cannot be neglected due to the fact that, the magnetic strength placed in a transverse direction within the channel undergo series of interactions especially in controlling hot moving fluid. For example [17], investigated the impact of magnetic source on nanofluid hydrothermal treatment in an enclosure with square hot cylinder. Also [18,19], considered the impact of induced magnetic field in the process of heat and mass transfer for nanofluid using Buongiorno model. In addition to that [20], examined the influence of magnetic field dependent (MFD) viscosity on MHD nanofield flow and heat transfer, thereby concluding that a reduction in heat transfer due to MFD viscosity is a rising function of Rayleigh number but a reducing function of magnetic strength parameter.

However, a lot of attention has been devoted to the study involving the impact of thermal radiation on fliud flow, like in Ref. [21], the study stated that it plays a vital role in the context of space technology and especially in a process involving high temperature. Other investigations that revealed the marked effect of thermal radiation, to mention few, are described in Refs. [16,18,19,21–25]. Also, the thermal stability analysis is another aspect of fluid flow that cannot be ignored because it gives information on the prediction of the critical or unsafe flow conditions as extensively explained in Ref. [26]. In support of this [27], studied

* Corresponding author. Department of Mathematical Sciences, University of South Africa, South Africa.
E-mail address: anthonyhassan72@yahoo.co.uk (A.R. Hassan).

http://dx.doi.org/10.1016/j.ijthermalsci.2017.08.022
1290-0729/

the steady state solutions for viscous reactive flows through channels with a sliding wall obtaining the analysis using a special type of Hermite–Padé approximation approach which has been proved extremely useful in the validation of purely numerical scheme. Other relevant studies showing the significance of thermal stability analysis can be found in Refs. [28–31].

Hence, the present study is to examine the thermodynamics analysis of a radiative heat transfer of a reactive hydromagnetic fluid through parallel porous plates under the effects of heat source and thermal radiation with convective boundary conditions following Newton's cooling law. This study also spreads out the recent work of [2–7] to examine the marked effect of thermal radiative heat transfer on the flow system with convective cooling of the walls using the modified Adomian decomposition method (MADM) to obtain the solutions of the momentum and energy equations governing the fluid flow. The choice of this method is due to the fact that, the method does not demand any linearization, discretization and use of guess or perturbation. This method, from literature has been proved to be efficient, reliable and a powerful tool in providing solution of differential and integral equations in a rapidly convergent series as discussed extensively in Refs. [32–36] and that it assures size-able savings in the computational volume. In addition to that, the analysis of thermal stability of the flow system is obtained using Padé approximation technique as obtained in Refs. [4–6,31].

In the rest of this paper, the mathematical model of the flow system are formulated in section 2. The non–linear equations for momentum and energy are solved in section 3 by making use of MADM and determine the entropy generation rate from the expressions of velocity and temperature profiles. The analysis of thermal stability is presented in section 4, the graphical presentation of results are shown in section 5 while the final conclusion was done in section 6.

2. Mathematical model

We consider a steady flow of an incompressible internal heat generating flow of a reactive hydromagnetic fluid within parallel porous plates of distance (2a) located at $y = -a$ and $y = a$ under the influence of radiative flux with convective cooling of the walls as depicted in the figure below (Fig. 1). In this present work, we neglect the consumption of the reactant of which the momentum and energy equations governing the fluid flow are given in non–dimensionless forms as mentioned in Refs. [2–5,10] may be written as:

$$\mu\frac{d^2\overline{u}}{d^2\overline{y}}\overline{u} - \frac{d\overline{P}}{d\overline{x}} - \frac{\mu}{K}\overline{u} - \sigma_0 B_0^2 = 0 \tag{1}$$

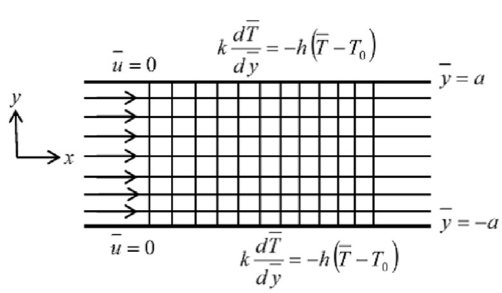

Fig. 1. The physical geometry of the flow regime.

$$k\frac{d^2\overline{T}}{d^2\overline{y}} + QC_0Ae^{-\frac{E}{RT}} + \mu\left(\frac{d\overline{u}}{d\overline{y}}\right)^2 + \frac{\mu}{K}\overline{u}^2 + \sigma_0 B_0^2\overline{u}^2 + Q_0\left(\overline{T} - T_0\right) - \frac{dq_r}{d\overline{y}} = 0 \tag{2}$$

with symmetric condition along the channel centreline given as

$$\frac{d\overline{u}}{d\overline{u}} = \frac{d\overline{T}}{d\overline{u}} = 0 \quad \text{on} \quad y = 0 \quad \text{and} \quad \overline{u} = 0, \quad k\frac{d\overline{T}}{d\overline{y}} = -h\left(\overline{T} - T_0\right) \quad \text{on} \quad y = a \tag{3}$$

such that P represents the pressure, T represents the fluid temperature, μ is known to be the fluid viscosity, u is the velocity, σ_0 represents electrical conductivity and K is Darcy's permeability constant, k represents the thermal conductivity coefficient, T_0 is the wall temperature, A is the constant of reaction rate, h is the heat transfer coefficient, Q is the heat of the reaction term, C_0 denotes the initial concentration of reactant species and E is the activation energy. In addition to that, R denotes the universal gas constant, Q_0 represent the dimensional heat generation coefficient and q_r denoted the radiative heat transfer flux.

The additional last term in the velocity equation (1) and the fifth term in energy equation (2) marked the impact of the magnetic field strength as in Refs. [2–8,17–20]. Moreso, the sixth term in energy equation (2) is the internal heat generation within the flow system as in Refs. [6,7,37,38] while the last term is the significant effect of radiative heat transfer fluid flow as described in Refs. [16,18,19,22–24]. The Rosseland approximation for thermal radiation is given as:

$$q_r = -\frac{4\sigma}{3k^*}\frac{d\overline{T}^4}{d\overline{y}} \tag{4}$$

such that σ denotes the Stefan-Boltzmann constant and k^* represent the mean absorption coefficient. A general assumption with the temperature difference for the flow system is such that T^4 may be expanded in Taylor series about the free-stream temperature, T_∞ and by neglecting the higher orders as done in Refs. [23,24] yield:

$$T^4 \equiv 4T_\infty^3 T - 3T_\infty^4 \tag{5}$$

such that

$$\frac{dq_r}{d\overline{y}} = -\frac{16\sigma T_\infty^3}{3k^*}\frac{d^2\overline{T}}{d\overline{y}^2} \tag{6}$$

However, the entropy generation rate (S^m), due to heat transfer under the influence of considerable radiative heat flux and the compound effects of fluid resistance on Joules dissipation, porous medium and magnetic field strength following [3,23,24,39–42] is given as:

$$S^m = \frac{k}{T_0^2}\left[\left(\frac{d\overline{T}}{d\overline{y}}\right)^2 + \frac{16\sigma T_\infty^3}{3kk^*}\left(\frac{d\overline{T}}{d\overline{y}}\right)^2\right] + \frac{1}{T_0}\left(\mu\frac{d\overline{u}^2}{d\overline{y}} + \frac{\mu}{K}\overline{u}^2 + \sigma_0 B_0\overline{u}^2\right) \tag{7}$$

We introduce these non-dimensional quantities in (1)–(7)

$$y=\frac{\bar{y}}{a},\quad x=\frac{\bar{x}}{a},\quad u=\frac{\bar{u}}{U},\quad T=\frac{E(\bar{T}-T_0)}{RT_0^2},\quad Br=\frac{E\mu U^2}{kRT_0^2},\quad \delta=\frac{RT_0}{E},$$

$$\Omega=\frac{1}{\delta},\quad \gamma=\frac{\mu U^2}{QAa^2C_0}e^{\frac{E}{RT_0}},\quad H^2=\frac{\sigma_0 B_0^2 a^2}{\mu},\quad G=-\frac{dp}{dx},\quad p=\frac{a\bar{p}}{\mu U},\quad \alpha=\frac{a^2}{K}$$

$$\lambda=\frac{QEAa^2C_0}{KRT_0^2}e^{-\frac{E}{RT_0}},\quad R_d=\frac{16\sigma T_\infty^3}{3kk^*},\quad Bi=\frac{ah}{k}\quad \text{and}\quad \beta=\frac{Q_0RT_0^2}{QAEC_0}e^{\frac{E}{RT_0}} \tag{8}$$

With (8) in (1)–(7), we obtain the following dimensionless boundary-valued problems:

$$\frac{d^2u}{dy^2}-\left(H^2+\alpha\right)u+G=0 \tag{9}$$

$$\frac{d^2T}{dy^2}+\frac{\lambda}{1+R_d}\left[e^{\frac{T}{1+\delta T}}+\gamma\left(\left(\frac{du}{dy}\right)^2+\left(H^2+\alpha\right)u^2\right)+\beta T\right]=0 \tag{10}$$

together with the boundary conditions

$$\frac{du}{dy}=\frac{dT}{dy}=0\quad \text{on}\quad y=0\quad \text{and}\quad u=0,\quad \frac{dT}{dy}=-BiT\quad \text{on}\quad y=1. \tag{11}$$

and the expression for the entropy generation rate in dimensionless form is compiled as:

$$N_s=\frac{S^mE^2a^2}{kR^2T_0^2}=\left(\frac{dT}{dy}\right)^2[1+R_d]+\frac{Br}{\Omega}\left[\left(\frac{du}{dy}\right)^2+\left(H^2+\alpha\right)u^2\right] \tag{12}$$

where G is the pressure gradient, U is the mean velocity and a denotes the channel half width. Also, Br represents the Brinkman number, Bi is the convective cooling term known as Biot number, H is the Hartmann number and N_s is the entropy generation rate. Other parameters in the expressions are $\lambda, R_d, \delta, \alpha, \gamma, \beta$ and Ω which respectively represent Frank–Kamenettski parameter, the conduction-radiation parameter, activation energy parameter, porous permeability parameter, viscous heating parameter, the heat source parameter and the wall temperature parameter.

3. Method of solution

The exact solution of momentum equation (9) with the appropriate boundary conditions is obtained to be:

$$u(y)=\frac{e^{-y\sqrt{\alpha+H^2}}\left(-e^{\sqrt{\alpha+H^2}}+e^{y\sqrt{\alpha+H^2}}+e^{(y+2)\sqrt{\alpha+H^2}}-e^{(2y+1)\sqrt{\alpha+H^2}}\right)G}{\left(e^{2\sqrt{\alpha+H^2}}+1\right)(\alpha+H^2)} \tag{13}$$

Moreover, the solution of the energy equation (10) shall be obtained by using modified Adomian decomposition method. Studied involving this technique can be found in Refs. [32–36,43,44]. Hence, the energy equation (10) is solved by introducing a second order linear operator $\Lambda(T)$ as:

$$\Lambda(T)=T(y)=\frac{d^2T}{dy^2}+\frac{\lambda}{1+R_d}\left[e^{\frac{T}{1+\delta T}}+\gamma\left(\left(\frac{du}{dy}\right)^2+\left(H^2+\alpha\right)u^2\right)+\beta T\right]=0 \tag{14}$$

such that:

$$\Lambda^{-1}=\int_0^y\int_0^y(\bullet)dy\,dy \tag{15}$$

However, introducing (15) into (14), we have

$$T(y)=d_0-\frac{\lambda}{1+R_d}\int_0^y\int_0^y\left[e^{\frac{T}{1+\delta T}}+\gamma\left(\left(\frac{du}{dy}\right)^2+\left(H^2+\alpha\right)u^2\right)+\beta T\right]dy\,dy \tag{16}$$

such that $d_0=T(0)$ and will be fixed on by using the boundary condition (11). The MADM demands that the inexact solution is given as a series solutions of

$$T(y)=\sum_{n=0}^{\infty}T_n(y) \tag{17}$$

The components $T_0, T_1, T_2, \ldots, T_k$ are to be determined. Thus, substituting (17) into (16) gives

$$T(y)=d_0-\frac{\lambda}{1+R_d}\int_0^y\int_0^y\left[e^{\frac{\left(\sum_{n=0}^{\infty}T_n(y)\right)}{1+\delta\left(\sum_{n=0}^{\infty}T_n(y)\right)}}+\gamma\left(\left(\frac{du}{dy}\right)^2+\left(H^2+\alpha\right)u^2\right)+\beta\left(\sum_{n=0}^{\infty}T_n(y)\right)\right]dy\,dy \tag{18}$$

The non–linear term in (18) can be presented by using the following series:

$$\sum_{n=0}^{\infty}A_n(y)=e^{\frac{\left(\sum_{n=0}^{\infty}T_n(y)\right)}{1+\delta\left(\sum_{n=0}^{\infty}T_n(y)\right)}} \tag{19}$$

where the Adomian polynomials, $A_0, A_1, A_2, \ldots, A_k$ are obtained by expanding (19) as follows:

$$A_0=e^{\frac{T_0(y)}{\delta T_0(y)+1}},$$

$$A_1=\frac{T_1(y)e^{\frac{T_0(y)}{\delta T_0(y)+1}}}{(\delta T_0(y)+1)^2},$$

$$A_2=\frac{e^{\frac{T_0(y)}{\delta T_0(y)+1}}\left(T_1(y)^2\left(-2\delta-2\delta^2T_0(y)+1\right)+2T_2(y)(\delta T_0(y)+1)^2\right)}{2(\delta T_0(y)+1)^4},\ldots, \tag{20}$$

and (18) is reduced to:

$$T(y)=d_0-\frac{\lambda}{1+R_d}\int_0^y\int_0^y\left[\sum_{n=0}^{\infty}A_n(y)+\gamma\left(\left(\frac{\mathrm{d}u}{\mathrm{d}y}\right)^2+\left(H^2+\alpha\right)u^2\right)+\beta\left(\sum_{n=0}^{\infty}T_n(y)\right)\right]\mathrm{d}y\,\mathrm{d}y \tag{21}$$

Taking the zeroth component of (21) as described in Refs. [33,34,36], the following are obtained:

$$T_0(y)=0 \tag{22}$$

$$T_1(y)=d_0-\frac{\lambda}{1+R_d}\int_0^y\int_0^y\left[A_0(y)+\gamma\left(\left(\frac{\mathrm{d}u}{\mathrm{d}y}\right)^2+\left(H^2+\alpha\right)u^2\right)+\beta T_0(y)\right]\mathrm{d}y\,\mathrm{d}y \tag{23}$$

$$T_{n+1}(y)=-\frac{\lambda}{1+R_d}\int_0^y\int_0^y[A_n(y)+\beta T_n(y)]\mathrm{d}y\,\mathrm{d}y\quad n\geq 1 \tag{24}$$

Hence, the solution to the energy equation is approximately obtained as

$$T(y)=\sum_{n=0}^{k}T_n(y) \tag{25}$$

With the help of Mathematica software package, equations (22)–(24) are programmed to secure the approximate solution of the energy equation. However, the respective solutions of momentum and energy equations in (13) and (25) are now used to analyze the entropy generation rates. For simplification, we separated the term in (7) into two as:

$$N_1=\left(\frac{\mathrm{d}T}{\mathrm{d}y}\right)^2[1+R_d]\ \text{and}\quad N_2=\frac{Br}{\Omega}\left[\left(\frac{\mathrm{d}u}{\mathrm{d}y}\right)^2+\left(H^2+\alpha\right)u^2\right] \tag{26}$$

where N_1 is the irreversibility heat transfer in the presence of appreciable radiative flux and N_2 is the local entropy generation due to the respective combined effects of viscous dissipation, magnetic field strength and porosity of the flow regime. Also, the irreversibility distribution ratio (ϕ) is define as

$$\phi=\frac{N_1}{N_2} \tag{27}$$

with an alternative irreversibility parameter, Bejan number (Be) defined as

$$Be=\frac{N_1}{N_s}=\frac{1}{1+\phi}\quad \text{where}\quad 0\leq Be\leq 1 \tag{28}$$

such that $Be=0$ when $N_2\gg N_1$, $Be=0.5$ when $N_1=N_2$ and $Be=1$ when $N_1\gg N_2$. The graphical results showing effects of various parameters on the rate entropy generation and Bejan number are displayed in Figs. (13–19).

4. Thermal stability analysis

The analysis of thermal criticality for fluid flow through a porous medium of a reactive hydromagnetic internal heat generating fluid under the impact of thermal radiation with convective cooling is obtained by using Padé approximation technique. The technique is a rational function that can be thought of as a generalization of a Taylor polynomials as described in Refs. [4–6,31] where the approximants are derived by expanding function as a ratio of two power series determining both the numerator and denominator coefficients. To this end, the diagonal form of the series solution (25) is evaluated using the built–in Padé approximant procedure in Mathematica with the boundary conditions in 13 given as:

$$T'(1)=-BiT(1) \tag{29}$$

Taking the diagonal Padé approximants $[M/M]$ of (29) at various values of M leads to an eigenvalue problem. This can be used to show the series convergence where the unknown constant (d_0) is evaluated using values for the known parameters. In the same way, the critical values of the Frank–Kamenettski parameter (λ_c) for the non–existence of the solution, or thermal runaway for the flow regime are obtained and shown in Table 2.

5. Discussion of results

In this part, the graphical representation of velocity profile in (13) and temperature profile in (25) which are used to obtain figures in investigating the impact of thermophysical parameter properties on a reactive hydromagnetic radiative heat transfer fluid flow within parallel porous plates with convective cooling walls are shown. Also, the solutions are used in (12) and (28) to obtain the graphical results for entropy generation rate and Bejan number.

Table 1 shows the rapid convergence of the series solution for the constant (d_0) in (25) and it showed that the series converge with size - able iterations. Table 2 demonstrates the thermal criticality values demonstrating the impacts of convective cooling and thermal radiation of the liquid stream. Eminently, the extent of thermal criticality increments with increasing values of Bi and R_d, therefore keeping the early improvement of thermal runaway, in this way, enhancing thermal dependability in the porous flow channels.

Figs. 2–4 display the velocity profile for variations in pressure

Table 1
Rapid convergence of the series solution for the constant (d_0).

$\beta=H=\delta=\lambda=0.1,\alpha=R_d=0.5,\gamma=G=1$	
n	d_0
0	0
1	0.047690
2	0.049549
3	0.049565
4	0.049565
5	0.049565

Table 2
Thermal criticality values showing the effects of convective cooling and thermal radiation.

Pade	G	H	δ	γ	β	α	R_d	Bi	λ_c
2/2	1	1	0.1	0.1	0.1	0.5	0.5	10	1.1481937089351166
2/2	1	1	0.1	0.1	0.1	0.5	0.5	15	1.2174970165922028
2/2	1	1	0.1	0.1	0.1	0.5	0.5	20	1.2551305810541624
2/2	1	1	0.1	0.1	0.1	0.5	0.1	10	0.8420087198857522
2/2	1	1	0.1	0.1	0.1	0.5	0.5	10	1.1481937089351166
2/2	1	1	0.1	0.1	0.1	0.5	1.0	10	1.5309249452468223

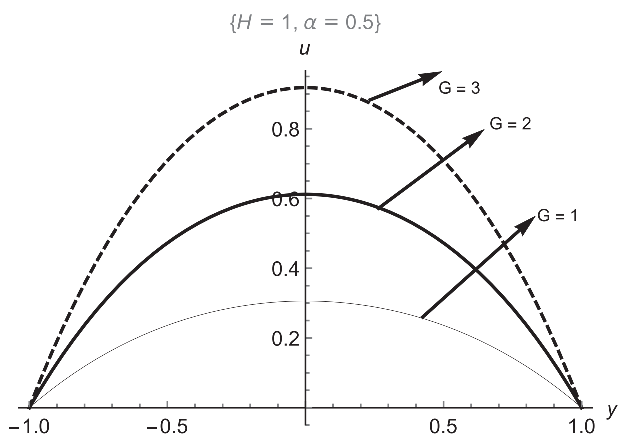

Fig. 2. Effects of G on $u(y)$.

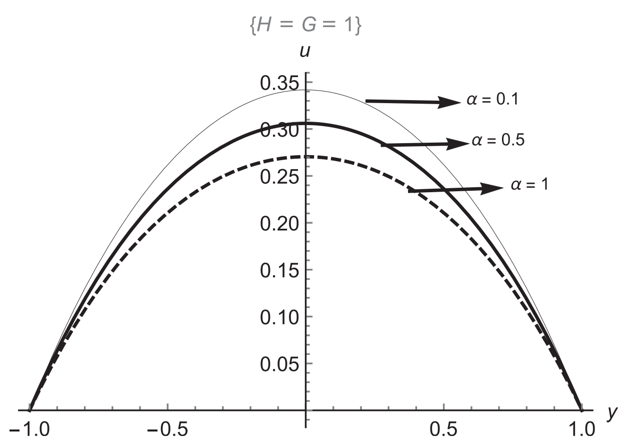

Fig. 3. Effects of α on $u(y)$.

gradient (G), the porous permeability parameter (α) and magnetic field parameter (H). Fig. 2 shows that the maximum velocity is obtained as the value of pressure gradient (G) increases, that is, the more the pressure is applied, the faster the fluid flow. But the reverse is recorded in Figs. 3 and 4, where a reduction is noticed as both the porous permeability parameter (α) and magnetic field parameter (H) increase. The delay in fluid flow is caused due to the presence of electromagnetic force and the resistance encountered within the porous channel of the flow regime.

The temperature distribution for different values of pressure gradient (G), viscous heating parameter (γ), internal heat generation parameter (β), Frank– Kamenettski parameter (λ), radiation parameter (R_d), porous permeability parameter (α), activation energy parameter (δ), Biot number (Bi) and magnetic field parameter (H) are respectively displayed in Figs. 5–12.

In Figs. 5–8, the maximum temperature is correspondingly

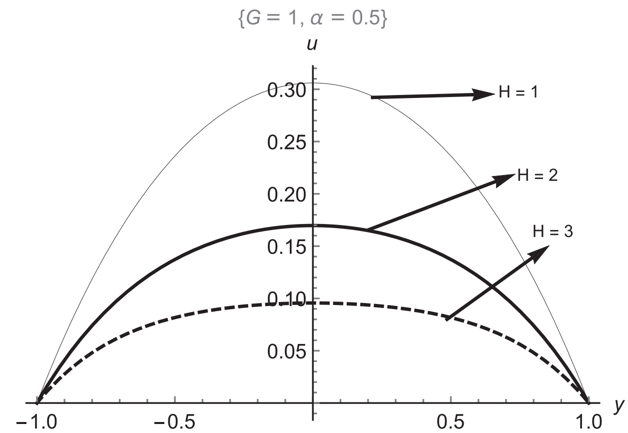

Fig. 4. Effects of H on $u(y)$.

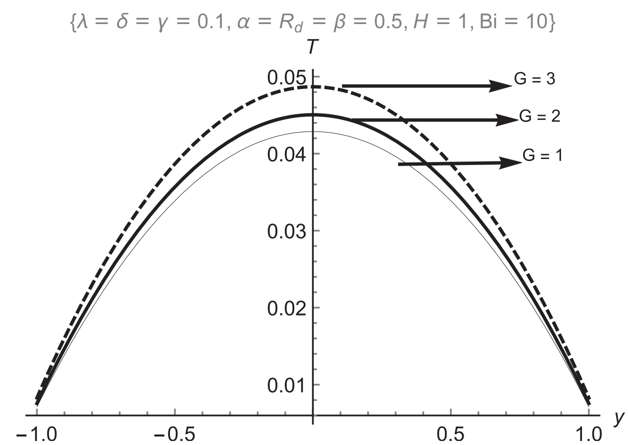

Fig. 5. Effect of G on $T(y)$.

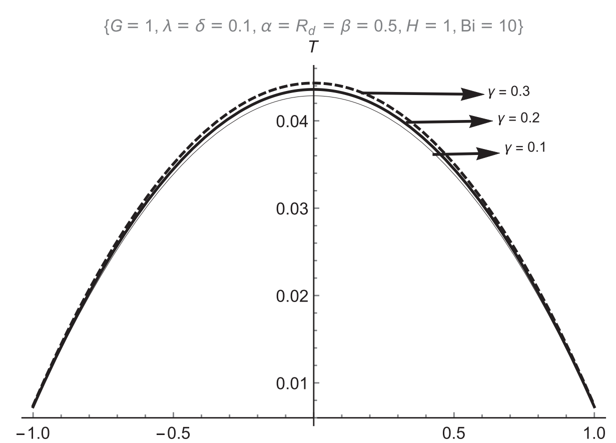

Fig. 6. Effect of γ on $T(y)$.

obtained at the maximum values of pressure gradient (G), viscous heating parameter (γ), heat source parameter (β) and Frank Kamenettski parameter (λ). This is actually true for the fact that the energy possessed by the fluid particles coupled with increase in pressure gradient (G) affect the fluid viscosity and internal energy producing heat due to particles interaction, hence, fluid temperature increases. Meanwhile, the contrary is noted in Figs. 9–12, where the maximum temperature is also recorded respectively for

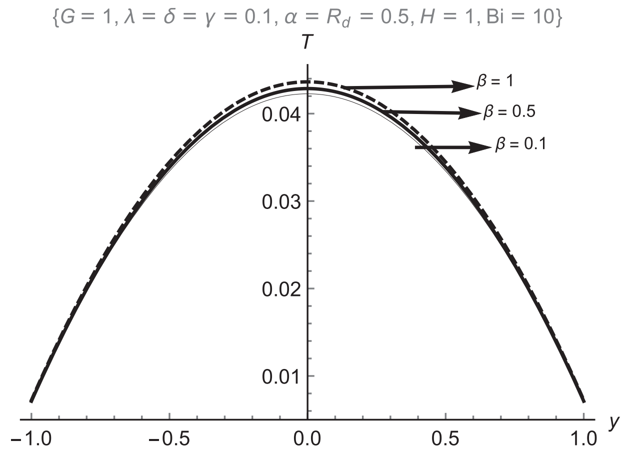

Fig. 7. Effect of β on $T(y)$.

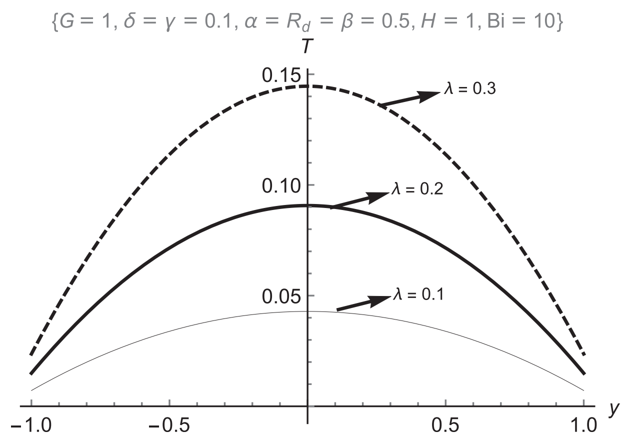

Fig. 8. Effect of λ on $T(y)$.

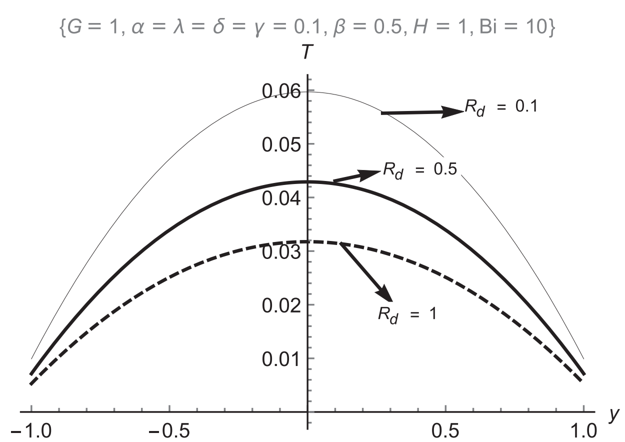

Fig. 9. Effect of R_d on $T(y)$.

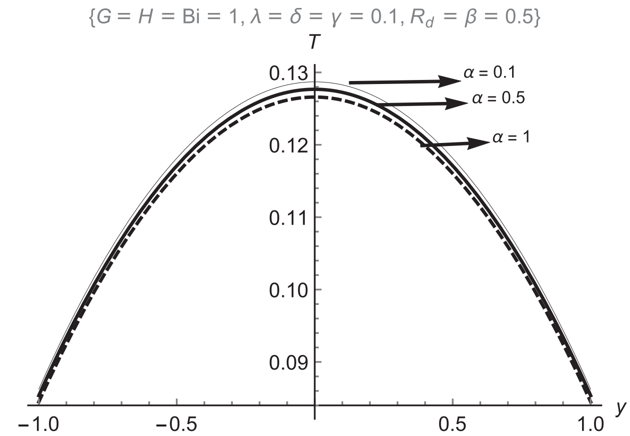

Fig. 10. Effect of α on $T(y)$.

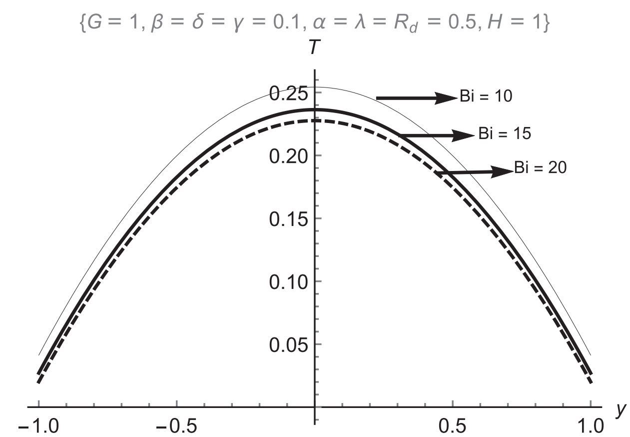

Fig. 11. Effect of *Bi* on $T(y)$.

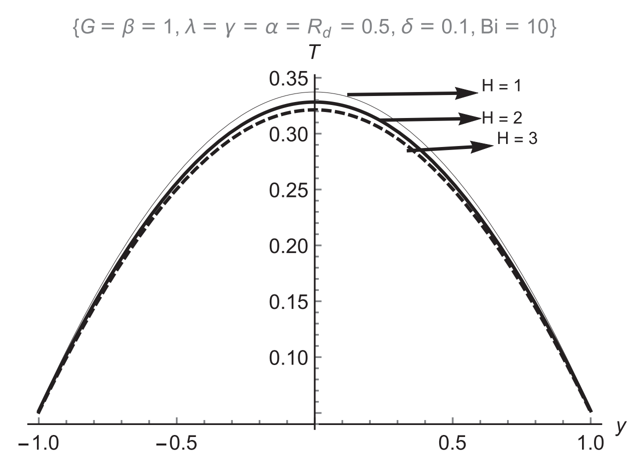

Fig. 12. Effect of *H* on $T(y)$.

the least value of radiation parameter (R_d), porous permeability parameter (α), Biot number (Bi) and magnetic strength parameter (H). The reason is that heat radiates through the porous medium from the centreline and there is convective cooling at the walls which reduces the amount of energy losses and allow the temperature to obtain an equilibrium that brings about reduction in the temperature.

The entropy generation analysis for variations in the convective cooling term (Bi), radiation parameter (R_d), Brinkman number (Br) and Frank–Kamenettski parameter (λ) are displayed in Figs. 13–16. The rate of entropy generation is active and at minimum around the centreline of flow channel and increases toward the walls. It is observed that the rate of entropy generation reduces at the channel walls with increasing values of both the Biot number (Bi) and radiation parameter (R_d) while the contrary is observed in the case of Brinkman number (Br) and Frank–Kamenettski parameter (λ)

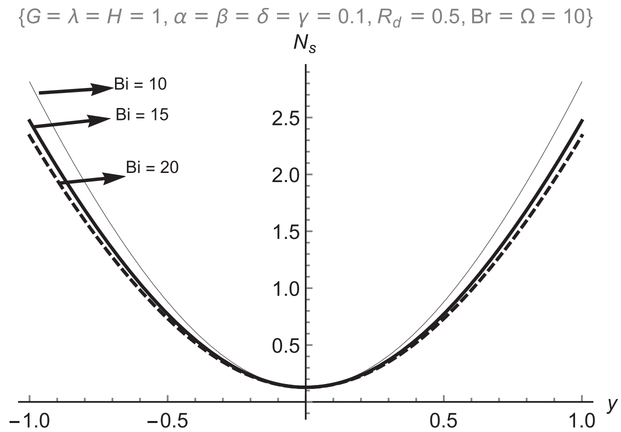

Fig. 13. Effect of Bi on N_s.

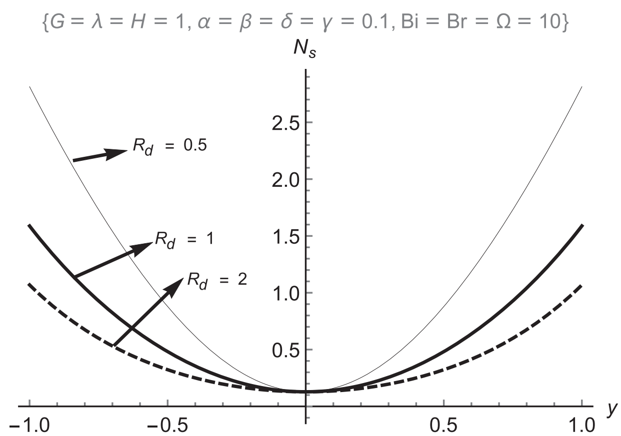

Fig. 14. Effect of R_d on N_s.

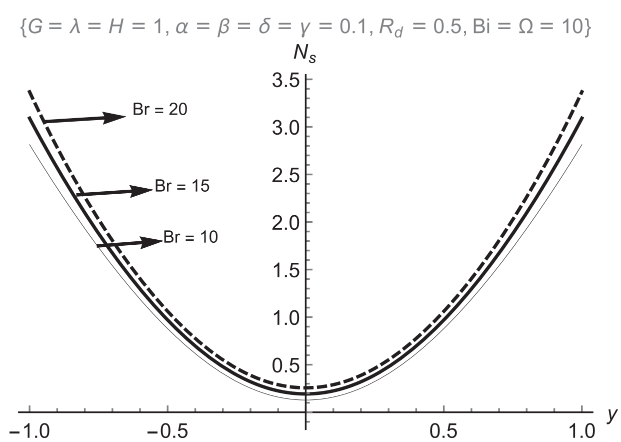

Fig. 15. Effect of Br on N_s.

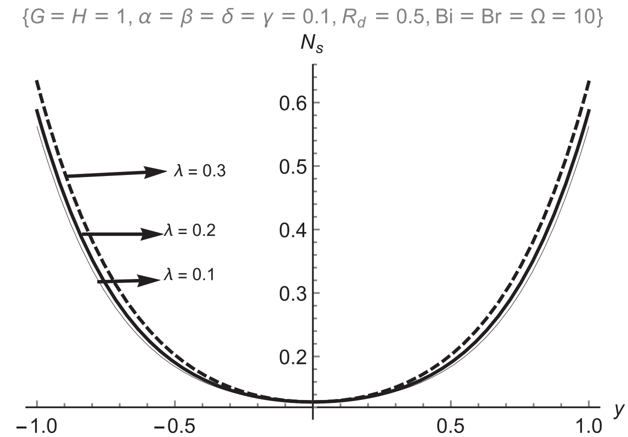

Fig. 16. Effect of λ on N_s.

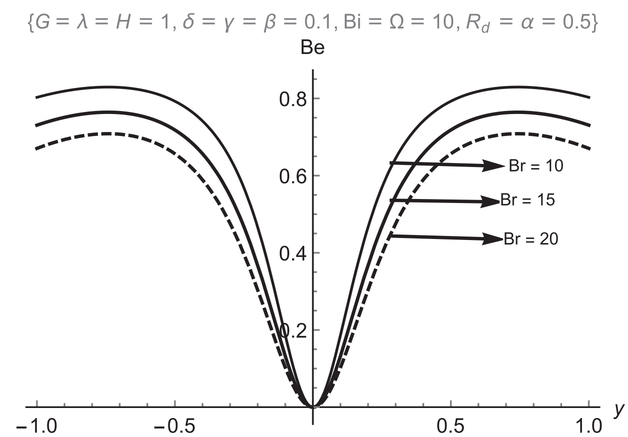

Fig. 17. Effect of R_d on Be.

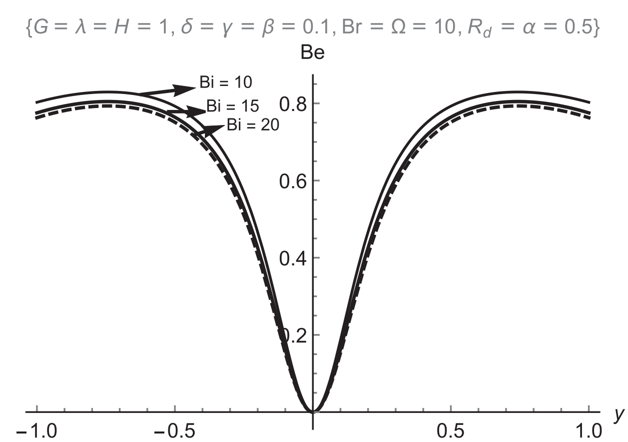

Fig. 18. Effect of Bi on Be.

where the entropy generation rate increases as (Br) and (λ) increase.

Effects of radiation parameter (R_d), convective cooling term, Biot number (Bi) and Brinkman number (Br) on Bejan numbers are displayed in Figs. 17–19. Here, it is noticed that fluid friction irreversibility increasingly dominates around the core region and heat transfer irreversibility dominates around the channel walls with increasing value of (R_d), (Bi) and (Br).

Fig. 20 displays a slice of bifurcation for λ, T_{Max} plane with Frank-Kamenetsski parameter. A turning point (λ_c) is a critical value such that, for $0 \le \lambda \le \lambda_c$, there exist upper and lower solutions (labelled I and II) which occur due to the chemical kinetics governing the solution of energy equations that are shown. This can also be seen in Table 2 where thermal criticality will give a rise if Bi and R_d are increased to prevent explosion in the flow regime.

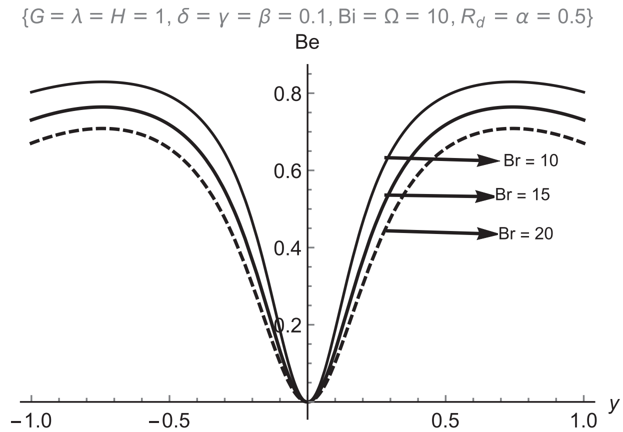

Fig. 19. Effect of *Br* on *Be*.

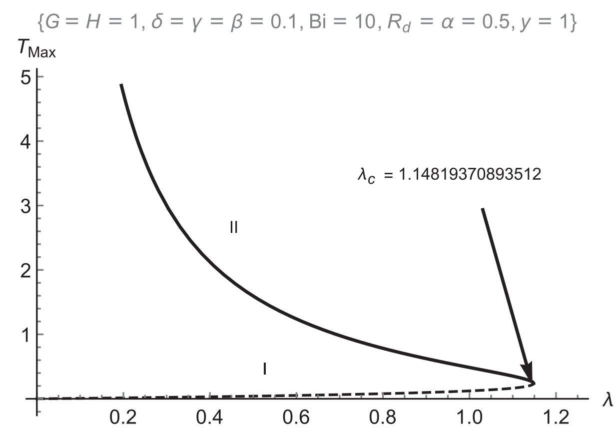

Fig. 20. A slice of approximate bifurcation for λ, T_{Max} plane.

6. Conclusion

The present study extends the recent work of [2–7] by investigating the impact of thermal radiation with convective boundary walls on a reactive hydromagnetic internal heat generating fluid flowing within porous medium. The dimensionless governing equations of the fluid flow are established using modified Adomian decomposition method (MADM) and the thermal stability analysis obtained using Padé approximation technique.

The results showed that the maximum velocity is obtained at the maximum value of pressure gradient (G) while a reduction is noticed as both the porous permeability parameter (α) and magnetic field parameter (H) increase. Also, the maximum temperature is recorded the maximum values of pressure gradient (G), viscous heating parameter (γ), heat source parameter (β) and the critical explosion parameter (λ) while the reverse is seen for the least value of radiation parameter (R_d), porous permeability parameter (α), activation energy parameter (δ), Biot number (Bi) and magnetic field parameter (H). However, the rate of entropy generation reduces at the channel walls with increasing values of both the convective cooling parameter (Bi) and radiation parameter (R_d). Also, it is noticed that fluid friction irreversibility increasingly dominates around the core region and heat transfer irreversibility dominates around the channel walls with increasing values of radiation parameter (R_d), convective cooling parameter (Bi) and Brinkman number as well.

Acknowledgment

The authors are thankful to the reviewers for their valuable suggestions to enhance the quality of this article.

Nomenclature

x, y	Coordinate system (m)
P	Pressure (Nm^{-2})
T	Temperature (K)
u	Velocity (ms^{-1})
h	Distance between the plates (m)
K	Darcy Permeability constant
k	Thermal conductivity coefficient $(Wm^{-1}K^{-1})$
R_d	Conduction-radiation parameter
N_s	Dimensionless entropy generation rate
C_0	Initial concentration of reactant species
Q_0	Dimensional heat generation coefficient
k^*	The mean absorption coefficient $(Wm^{-1}K^{-1})$
q_r	Radiative heat transfer flux (Wm^{-2})
h	Heat transfer coefficient
a	Channel half width (m)
Br	Brinkman number
Bi	Biot number
H	Hartmann number
T_0	Wall temperature (K)
A	Reaction rate constant
Be	Bejan Number
E	Activation energy
R	Universal gas constant
U	Mean velocity (ms^{-1})
G	Pressure gradient(Nm^{-2})
S^m	Entropy generation rate
Q	Heat of the reaction term

Greek symbols

α	Porous permeability parameter
σ	Stefan-Boltzmann constant $(Wm^{-2}K^{-4})$
(ϕ)	The irreversibility distribution ratio
λ	Frank–Kamenettski parameter
γ	Viscous heating parameter
β	Heat source parameter
σ_0	Electrical conductivity
μ	Fluid viscosity (m^2s^{-1})
δ	Activation energy parameter
Ω	Wall temperature parameter

References

[1] Akhtar W, Fetecau C, Tigoiu V, Fetecau C. Flow of a maxwell fluid between two side walls induced by a constantly accelerating plate. Z für Angew Math Phys 2009;60(3):498–510.
[2] Makinde OD, Ãnwar Beg O. On inherent irreversibility in a reactive hydromagnetic channel flow. J Therm Sci 2010;19(1):72–9.
[3] Hassan AR, Gbadeyan JA. Entropy generation analysis of a reactive hydromagnetic fluid flow through a channel. U P B Sci Bull Ser A 2015;77(2):285–96.
[4] Hassan AR, Maritz R. The analysis of a reactive hydromagnetic fluid flow in a channel through porous medium with convective cooling. U P B Sci Bull Ser D 2016;78(4):43–56.
[5] Hassan AR, Gbadeyan JA. Thermal stability analysis of a reactive hydromagnetic fluid flow through a channel. Am J Appl Math 2014;2(1):14–20.
[6] Hassan AR, Maritz R. The analysis of a reactive hydromagnetic internal heat generating poiseuille fluid flow through a channel. SpringerPlus 2016;5(1):1–14.
[7] Hassan AR, Gbadeyan JA. A reactive hydromagnetic internal heat generating fluid flow through a channel. Int J Heat Technol 2015;33(3):43–50.
[8] Krishnamurthy MR, Prasannakumara BC, Gireesha BJ, Gorla RSR. Effect of viscous dissipation on hydromagnetic fluid flow and heat transfer of nanofluid over an exponetially stretching sheet with fluid-particle suspension. Cogent

Math 2015;2:1–18.

[9] Hassan AR, Maritz R. The analysis of a variable-viscosity fluid flow between parallel porous plates with non-uniform wall temperature. Italian J Pure Appl Math 2016;36:1–12.

[10] Makinde OD. Thermal stability of a reactive viscous flow through a porous-saturated channel with convective boundary conditions. Appl Therm Eng 2009;29(8):1773–7.

[11] Makindel OD. On thermal stability of a reactive third-grade fluid in a channel with convective cooling the walls. Appl Math Comput 2009;213(1):170–6.

[12] Olanrewaju PO, Gbadeyan JA, Hayat T, Hendi AA. Effects of internal heat generation, thermal radiation and buoyancy force on a boundary layer over a vertical plate with a convective surface boundary condition. South Afr J Sci 2011;107(9–10):80–5.

[13] Mukhopadhyay S, Layek GC. Effects of thermal radiation and variable fluid viscosity on free convective flow and heat transfer past a porous stretching surface. Int J Heat Mass Transf 2008;51(9):2167–78.

[14] Mukhopadhyay S. Effects of thermal radiation and variable fluid viscosity on stagnation point flow past a porous stretching sheet. Meccanica 2013;48(7):1717–30.

[15] Vyas P, Srivastava N. Entropy analysis of generalized mhd couette flow inside a composite duct with asymmetric convective cooling. Arabian J Sci Eng 2015;40(2):603–14.

[16] Srinivasacharya D, Mendu U. Thermal radiation and chemical reaction effects on magnetohydrodynamic free convection heat and mass transfer in a micropolar fluid. Turkish J Eng Environ Sci 2015;38(2):184–96.

[17] Sheikholeslami M, Ganji DD. Free convection of fe 3 o 4-water nanofluid under the influence of an external magnetic source. J Mol Liq 2017;229:530–40.

[18] Sheikholeslami M, Ganji DD. Nanofluid hydrothermal behavior in existence of lorentz forces considering joule heating effect. J Mol Liq 2016;224:526–37.

[19] Sheikholeslami M, Ganji DD, Rashidi MM. Magnetic field effect on unsteady nanofluid flow and heat transfer using buongiorno model. J Magnetism Magnetic Mater 2016;416:164–73.

[20] Sheikholeslami M, Rashidi MM, Hayat T, Ganji DD. Free convection of magnetic nanofluid considering mfd viscosity effect. J Mol Liq 2016;218:393–9.

[21] Krishnamurthy MR, Gireesha BJ, Prasannakumara BC, Gorla RSR. Thermal radiation and chemical reaction effects on boundary layer slip flow and melting heat transfer of nanofluid induced by a nonlinear stretching sheet. Nonlinear Eng 2016;5(3):147–59.

[22] Mukhopadhyay S. Effects of radiation and variable fluid viscosity on flow and heat transfer along a symmetric wedge. J Appl Fluid Mech 2009;2(2):29–34.

[23] Chauhan DS, Khemchandani V. Entropy generation in the poiseuille flow of a temperature dependent viscosity fluid through a channel with a naturally permeable wall under thermal radiation. Adv Appl Sci Res 2016;7(4):104–20.

[24] Yang Y, Chang K, Chen C. Entropy generation of radiation effect on laminar-mixed convection along a wavy surface. Heat Mass Transf 2011;47(4):385–95.

[25] Sheikholeslami M, Ganji DD, Javed MY, Ellahi R. Effect of thermal radiation on magnetohydrodynamics nanofluid flow and heat transfer by means of two phase model. J Magnetism Magnetic Mater 2015;374:36–43.

[26] Makinde OD. Thermal criticality for a reactive gravity driven thin film flow of a third-grade fluid with adiabatic free surface down an inclined plane. Appl Math Mech 2009;30(3):373–80.

[27] Makinde OD. Thermal criticality in viscous reactive flows through channels with a sliding wall: an exploitation of the hermite–padé approximation method. Math Comput Model 2008;47(3):312–7.

[28] Makinde OD. Thermal stability of a reactive viscous flow through a porous-saturated pipe. Int J Numer Methods Heat Fluid Flow 2007;17(8):836–44.

[29] Makinde OD. Irreversibility analysis of variable viscosity channel flow with convective cooling at the walls. Can J Phys 2008;86(2):383–9.

[30] Makinde OD. Thermal analysis of a reactive generalized couette flow of power law fluids between concentric cylindrical pipes. Eur Phys J Plus 2014;129(12):1–9.

[31] Adesanya SO. Thermal stability analysis of reactive hydro-magnetic third grade fluid through a channel with convective cooling. J Niger Math Soc 2013;32:61–72.

[32] Wazwaz AM. The modified adomian decomposition method for solving linear and nonlinear boundary value problems of tenth-order and twelfth-order. Int J Nonlinear Sci Numer Simul 2000;1(1):17–24.

[33] Wazwaz AM, El-Sayed SM. A new modification of the adomian decomposition method for linear and nonlinear operators. Appl Maths Comput 2001;122:393–405.

[34] Babolian E, Biazar J. Solution of nonlinear equations by modified adomian decomposition method. Appl Math Comput 2002;132(1):167–72.

[35] Wazwaz AM. A reliable modification of adomian decomposition method. Appl Math Comput 1999;102(1):77–86.

[36] Wazwaz AM. A new algorithm for calculating adomian polynomials for nonlinear operators. Abstr Appl Analysis 2000;111(1):53–69.

[37] Jha BK, Ajibade AO. Free convective flow of heat generating/absorbing fluid between vertical porous plates with periodic heat input. Int Commun Heat Mass Transf 2009;36(6):624–31.

[38] El-Amin MF. Combined effect of internal heat generation and magnetic field on free convection and mass transfer flow in a micro polar fluid with constant suction. J Magnetism Magnetic Mater 2004;270:130–5.

[39] Woods LC. The thermodynamics of fluid systems. Oxford: Oxford University Press; 1975.

[40] Bejan A. Entropy generation minimization: the method of thermodynamic optimization of finite-size systems and finite-time processes. CRC press; 1995.

[41] Bejan A. Fundamentals of exergy analysis, entropy generation minimization, and the generation of flow architecture. Int J energy Res 2002;26(7):0–43.

[42] Butt AS, Ali A. Entropy analysis of flow and heat transfer caused by a moving plate with thermal radiation. J Mech Sci Technol 2014;28(1):343–8.

[43] Ray SS. New approach for general convergence of the adomian decomposition method. World Appl Sci J 2014;32(11):2264–8.

[44] Hosseini MM, Nasabzadeh H. On the convergence of adomian decomposition method. Appl Math Comput 2006;182(1):536–43.